Int J Biometeorol (1995) 38:209–215


ORIGINAL ARTICLE

K-P. Wittich · O. Hansing

# Area-averaged vegetative cover fraction estimated from satellite data

Received: 30 September 1994 / Revised 3 January 1995 / Accepted: 4 January 1995

**Abstract** The relationship was analysed between the vegetation cover factor expressed as a percentage and the area-averaged normalized difference vegetation index (NDVI). On selected days the NDVI was calculated from channel 1 and 2 reflectance data of the National Oceanic and Atmospheric Administration (NOAA–11) satellite's advanced very high-resolution radiometer (AVHRR) for five test areas under agricultural and forestry use. No ground-based reflectance measurements could be made for validation of these data. Therefore the land surface NDVI, which varied with time, and percentage vegetation cover of the test areas were deduced from time-independent but site-specific statistical land use data updated by temporal phenological observations, and from surface-specific reflectance curves published in the literature. The result indicated that the area-averaged NDVI, as obtained from the NOAA–11 radiometer, was less than the value calculated from the land surface NDVI. After correction to reduce the offset of the data, the values would be a suitable indicator of the fraction of vegetation cover.

**Key words** Vegetation cover factor · Normalized difference vegetation index · Phenological data

## Introduction

Land surface studies are becoming more and more important due to increasing anthropogenic influences on natural biogenic resources, such as water, soil, vegetation and air. Indicators for anthropogenic effects on the planet earth include the trends of atmospheric concentrations of greenhouse gases, e.g. $CO_2$, and consequently in air temperature or precipitation trends. Further anthropogenic effects can be identified in anomalies in the temporal behaviour of vegetation. Variations in vegetative land cover occur in two ways: firstly, the annuals may vary according to season with a more or less distinct long-term phenological trend induced by climatic change, i.e. with an annual premature or belated occurrence of phenological stages in relation to 30-year averages. Secondly, vegetative cover may abruptly change due to human short-term activities in the biosphere, e.g. due to deforestation, changes in agricultural land use, urbanization or pollution.

Vegetation plays an important role in the exchange of energy at the land surface, in the biogeochemical cycle and in the hydrological cycle. Concerning the last-mentioned aspect, stomata regulate the water vapour flux from the plant interior to the atmosphere depending on the existing biological, hydrological and meteorological conditions. Furthermore, leaves intercept rainwater according to the plant-specific water-holding capacity; thus only a fraction of the precipitation observed in the open can reach the earth's surface, where it moistens the soil and may produce runoff. The partition of a defined area into vegetated and non-vegetated sub-areas is therefore an important aspect of land-surface modelling.

To enhance our understanding of environmental events and processes, the biological and physical characteristics of land surfaces must be measured and classified, in order to provide input to hydro-, meteorological, ecological and other models. Data are generally required about land-surface characteristics on a range of scales and often at several different times of year. Monitoring of the land surface can be done by ground-based observers and by remote sensing systems mounted on aircraft or satellites. Remote sensing data provide radiation characteristics from the land surface at well-defined spatial and temporal resolutions. For this reason multispectral data are of some use in assessing the area-averaged biophysical activity of vegetation.

In this study reflectance data from the advanced very high-resolution radiometer (AVHRR) mounted on the National Oceanic and Atmospheric Administration (NOAA-11) satellite have been used to assess the percentage vegetation cover as an important component of vegetation dynamics. Because it was necessary to quanti-

K-P. Wittich, (✉) · O. Hansing
Deutscher Wetterdienst,
Zentrale Agrarmeteorologische Forschungsstelle, Bundesallee 50,
D-38116 Braunschweig, Germany

fy the relationship between the land-surface function and spectral land-surface signatures, the so-called normalized difference vegetation index (NDVI) was applied. The NDVI changes in magnitude according to the nature of the land surface cover, which is variable in space and time. Different surfaces generally have different reflectivities in different parts of the spectrum and therefore produce different NDVIs (see the cover-type stratification of NOAA-7 NDVI responses in Table 1 of Holben (1986)).

## Methods

### NDVI and NOAA-AVHRR data

The NDVI is commonly used as a greenness parameter which indicates the biophysical activity of the land surface. The NDVI itself is defined by a combination of the reflected near-infrared and visible radiation according to

$$\mathrm{NDVI} = \frac{r^{\mathrm{NIR}} - r^{\mathrm{VIS}}}{r^{\mathrm{VIS}} + r^{\mathrm{NIR}}} \quad (1)$$

where $r^{\mathrm{NIR}}$ and $r^{\mathrm{VIS}}$ are surface reflectances for the near-infrared (NIR) and visible (VIS) wavelength intervals, respectively. Figure 1 shows spectral reflectance curves of different surfaces in the VIS and NIR spectral bands. Each surface has a specific spectral signature by which it can be more or less identified.

The magnitude of the NDVI also depends on the spectral resolution of the radiometer. In this study multispectral data from channels 1 and 2 of the AVHRR of the polar orbiting NOAA-11 satellite were used. Channel 1 operated in the visible range where chlorophyll absorption takes place, channel 2 in the near-infrared range where mesophyll reflectivity of the leaves is strong. Figure 1 shows the relative spectral responses of the NOAA-AVHRR sensor. Only integrated reflectivities over the wavelength bands used in the scanner were obtainable. In addition, spatial averaging took place inside each pixel over an area characterized by a typical dimension of 1.1*1.1 km$^2$ at nadir. Nevertheless, the sensor system of the NOAA-AVHRR has been thought to be suitable for biophysical tasks (Sellers 1987; Sellers et al. 1992). Global monitoring of vegetation using channel 1 and 2 data of the NOAA satellite has been done by Justice et al. (1985) among others, while Blümel et al. (1988) have used this satellite for calculating the NDVI for different parts of Europe, especially for Germany. In our study NOAA data of five test areas in western Germany with different types of land cover were analysed.

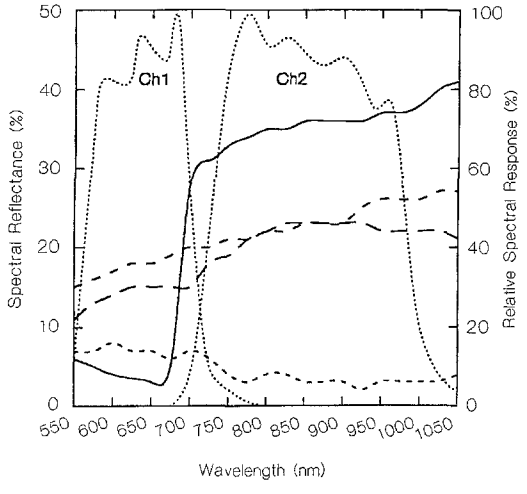


**Fig. 1** Spectral reflectance curves in the visible and near-infrared wavelengths for different land surface covers, and the response function of channels 1 and 2 (Ch1 and Ch2) of the advanced very high-resolution radiometer (AVHRR) (after Blümel et al. 1988). ---- water; – – – soil; — — stubble field; ——grass

### Data selection, test sites and NDVI verification procedure

Land-surface observations with optical sensors require cloudless conditions. For this reason, the study was based on up to 18 selected days between May 1992 and May 1993 with good remote sensing weather. Only afternoon overpasses of NOAA-11 (12:40 UTC – 14:30 UTC, UTC Universal Time Coordinated) were analysed. Although a geographical fine adjustment of the picture elements in relation to ground targets was made, there was an uncertainty in the spatial accuracy of NOAA-satellite picture elements of ±1 pixel. For this reason no validation for each single pixel was made in the following investigation. On the contrary, the pixel scale was enlarged to a regional scale of a site-specific order of 10 km$^2$, and area averaging was then done to obtain representative information.

To check the NOAA-NDVI data against land-surface values and to establish a simple formula for assessing the vegetation cover from the NDVI as subsequently described, five test areas of 9–35 km$^2$ in size (equal to a set of 9–35 pixels) and with different types of land cover were chosen in western Germany. These areas were Wesermarsch (08° 24′ E, 53° 16′ N) covered by grassland, Altes Land (09° 45′ E, 53° 30′ N), Hildesheimer Börde (10° 07′ E, 52° 14′ N) and Alzeyer Hügelland (08° 12′ E, 49° 45′ N) used for fruit-growing, arable farming and vine-growing, respectively,

**Table 1** Land use classification of five test sites

| Test site | Land use portions (%) |
|---|---|
| Wesermarsch | 96 Grassland<br>02 Water<br>02 Concrete |
| Altes Land | 75 Apple orchards<br>10 Cherry orchards<br>10 Grass<br>03 Deciduous forests<br>02 Water |
| Hildesheimer Börde | 28 Wheat<br>20 Sugar-beet<br>15 Mixed canopies<br>14 Barley<br>10 Soil<br>05 Concrete<br>03 Asphalt<br>02 Rye<br>02 Potato growing<br>01 Fallow/waste land |
| Rheinhessen | 50 Vineyards<br>20 Grass<br>10 Wheat<br>10 Soil<br>04 Sugar-beet<br>02 Rye<br>02 Asphalt<br>01 Fallow/waste land<br>01 Concrete |
| Pfälzer wald | 37 Pine trees<br>25 Copper beech<br>12 Spruce<br>12 Oak trees<br>09 Deciduous forests<br>05 Asphalt |

and Pfälzer Bergland (07° 50′ E, 49° 19′ N) covered with forest stands. The typical land cover portions for the test regions (Table 1) were obtained from agricultural, forestry and statistical agencies. The data of Table 1 indicate that the land surface of the test areas was spatially heterogeneous, i.e. most of the test areas contained vegetation of non-uniform physiology, leaf geometry and spectral properties.

For validation the NOAA-NDVIs should be compared with data obtained on the ground. Unfortunately, no ground-based measurements could be performed. Therefore spectral reflectance curves of a variety of site-specific types of land cover were taken from the literature (Kadro 1981; Huss 1985; Bowker et al. 1985; Szasz 1986; Blümel et al. 1988; Buschmann and Stützel 1993) and averaged over the range of AVHRR channel 1 and channel 2 windows to construct a synthetic land surface NDVI for validation. The resulting magnitude of the synthetic NDVI was 0.7 for green biomass, 0.15 for bare soil and less than zero for water. The NDVI of the annuals depends on their phenological stage; e.g. the canopy NDVI of wheat reaches somewhere in the region of 0.55 during emergence, 0.75 during shoot development, 0.3 during flowering and 0.05 during yellow ripening. A stubble field produces a canopy NDVI of approximately 0.17.

Some of the vegetation-related reflectance curves needed for analysis could not be found in the literature. In particular, there was a lack of data for different stages of the vegetation cycle of most plants. In other cases auxiliary reflectance curves were established, e.g. the unknown signal for deciduous trees was constructed from known signals of beech and oak trees, and the signal of fallow and waste land was represented by stubble-field reflectances.

To adjust the synthetic time-independent land surface information (Table 1) to seasonal vegetation dynamics, actual ground-based phenological observations of the phenological network of the Deutscher Wetterdienst (DWD) were employed. These data indicated the time of onset of new stages in plant development. Using this information it was possible to simulate the seasonal changes of greenness as a first approximation. This was done in two ways: the first was to choose from the literature the available synthetic reflectance curves of the actual plant development, e.g. those of emergence, shoot development, flowering etc. for wheat growth. The second method was applied when the reflectance curves for special phenophases were missing. In this case, the statistical cover portions of Table 1 were changed empirically in agreement with the observed phenological plant development. For example when leaf fall was reported by phenological observers the cover fraction of deciduous trees was diminished drastically and the soil cover portion (as a rough auxiliary parameter for dead organic matter) was augmented to bring the wooded area to its statistical total cover portion. When grassland dried out and its greenness was followed by yellowing, the statistical cover fraction of grassland was reduced and equilibrated by that of a stubble-field as an auxiliary value. Further discussion on this aspect is given later.

To adapt the information content of synthetic subscale albedos or pixel-scale NOAA reflectivities to a regional scale, a spatial average was calculated inside each test area. This resulted in a simple mean NOAA-NDVI value per test site while the synthetic land-surface analogue was calculated according to Eq. (1) from the weighted sum of the individual albedos, $r_i^\lambda$, of $n$ subregions, i.e.

$$r^\lambda = \sum_{i=1}^{n} r_i^\lambda \frac{A_i}{A} \tag{2}$$

with

$$\sum_{i=1}^{n} \frac{A_i}{A} = 1 \tag{3}$$

where $A_i$=$A_1$, $A_2$, ... $A_n$ are the dimensions of the land cover sub-areas, $A$ is the total size of the experimental test region and $A_i/A$ is the cover fraction of a vegetation class defined in Table 1. The index $\lambda$ corresponds to an average over the channel 1 or channel 2 wavelength intervals of the AVHRR sensor.

Plant cover factor

To assess the fraction of vegetation cover of the test areas, we took as a basis the statistical land cover data which were updated by phenological corrections, as described in the foregoing section. All the sub-surfaces which consisted of bare soil, asphalt, concrete, water, fallow, waste land and dead organic matter (e.g. soil and stubble field signatures as auxiliary values) were declared as non-vegetated. Deciduous wood, for example, which is integrated within the vegetated area during the vegetational period, was classified as a non-vegetated area after phenologically reported shedding of leaves and during winter dormancy.

Empirical σ-NDVI relationship

The approximation of the vegetational cover fraction, $\sigma$, follows the idea of Deardorff (1978), who considered a so-called area-averaged shielding factor for the case of land-surface heterogeneity in surface-vegetation-atmosphere-transfer (SVAT) models. This shielding factor is defined as the degree to which the foliage prevents shortwave radiation from reaching the ground. It extends from the case of no shielding of the ground by vegetation to complete shielding ($0 \le \sigma \le 1$). The lower boundary, $\sigma$=0, designates no foliage or bare ground, the upper, $\sigma$=1, complete radiative blocking of the ground by leaves, and therefore total vegetational cover.

Deardorff (1978) used a linear interpolation of the general form

$$\phi = (1-\sigma)*\phi_{\sigma=0} + \sigma*\phi_{\sigma=1} \tag{4}$$

to combine the effects of bare ground-related variables, $\phi_{\sigma=0}$, and vegetation-related variables, $\phi_{\sigma=1}$. In his study he applied this formula to heat and moisture transfer coefficients, to state variables of in-canopy flow, and to radiational components, so that the resultant energy fluxes could be described as a function of fractional vegetation cover. The basic idea of using an area-averaged foliage shielding factor has been followed here. This factor has been defined more generally as an area-averaged weighting factor which varies between $\sigma$=0 for bare soil and dead organic matter and $\sigma$=1 for 100% living organic matter.

Commonly it has been assumed that the plant cover fraction affects the NDVI response (Sellers 1985; Blümel et al. 1988; Carlson et al. 1990). An empirical working hypothesis has been that this factor can be described as a linear function of the normalized difference vegetation index, NDVI, according to

$$\sigma = a*\mathrm{NDVI} + b \tag{5}$$

with

$$a = \frac{1}{\mathrm{NDVI}_{\sigma=1} - \mathrm{NDVI}_{\sigma=0}}, \quad b = -\frac{\mathrm{NDVI}_{\sigma=0}}{\mathrm{NDVI}_{\sigma=1} - \mathrm{NDVI}_{\sigma=0}} \tag{6}$$

Here $\mathrm{NDVI}_{\sigma=0}$ is that index which is produced by non-living organic matter or bare soil, e.g. by land surfaces able to evaporate water but not to transpire it, while $\mathrm{NDVI}_{\sigma=1}$ is produced by a dense transpiring green canopy. Rewriting Eqs. (5) and (6) gives

$$\mathrm{NDVI} = (1-\sigma)*\mathrm{NDVI}_{\sigma=0} + \sigma*\mathrm{NDVI}_{\sigma=1} \tag{7}$$

which is identical to the form of Eq. (4) with $\phi$=NDVI.

An alternative formula describing the vegetative cover fraction is based on the relation

$$r^\lambda = (1-\sigma)*r_{\sigma=0}^\lambda + \sigma*r_{\sigma=1}^\lambda \tag{8}$$

where the wavelength $\lambda$ stands for the VIS and NIR range of AVHRR channels 1 and 2. Equation (8) conforms to that used by Blümel et al. (1988) or Manzi and Planton (1994).
When Equation (8) is included in Eq. (1) the result is

$$\sigma = \frac{c*\mathrm{NDVI} - d}{e*\mathrm{NDVI} + f} \tag{9}$$

with

$$c = r_{\sigma=0}^{\mathrm{Ch1}} + r_{\sigma=0}^{\mathrm{Ch2}}, \; d = r_{\sigma=0}^{\mathrm{Ch2}} - r_{\sigma=0}^{\mathrm{Ch1}}, \; e = c - r_{\sigma=1}^{\mathrm{Ch1}} - r_{\sigma=1}^{\mathrm{Ch2}}, \; f = -d + r_{\sigma=1}^{\mathrm{Ch2}} - r_{\sigma=1}^{\mathrm{Ch1}} \tag{10}$$

## Results

### Case study

Fig. 2 portrays, as an example, the seasonal vegetative phenological cycle of the NDVI in one of the five test areas, the Rheinhessen area, between May 1992 and April 1993. The curves are based on NOAA-AVHRR data from 13 images, and on synthetic data derived from statistical land cover values, which were updated by empirical assumptions based on phenological observations. The statistical land cover classification of this area gave 50% land cover for vineyards, 20% for grass, 10% for wheat fields etc. (see Table 1 and first line of Table 2).

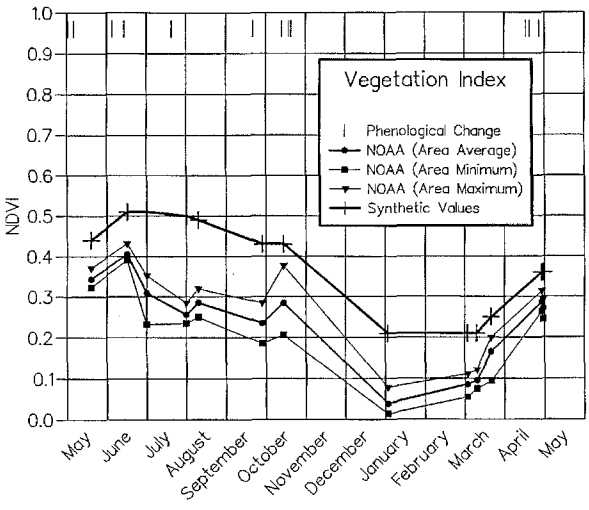


**Fig. 2** Annual course of the normalized difference vegetation index (NDVI) of the National Oceanic and Atmospheric Administration (NOAA–11) satellite for the Rheinhessen test area (area average, absolute maximum and minimum) and area-averaged synthetic canopy NDVI as given in Table 2 for May 1992–April 1993. The *vertical lines* near the top indicate the beginning of relevant phenological developments

The following modification of the statistical land-cover classification was made to obtain time-varying cover portions and time-dependent weighting factors in order to assess the temporal course of land surface albedos: on 18.5.92, the day of the first chosen overpass and 12 days after vine leaf unfolding, 30% of the total area was assumed to be covered by photosynthetically active green vine leaves and representing 20% less than the statistical optimum. The remaining 20% portion was classified as poor soil found in the rows between the vines. About 1 month later during the period when the vines flowered, all the vineyards were assumed to be covered by leaves. At the same time the soil cover portion was reduced by 20%. An additional reduction of the soil area by 1% resulted from the closing of sugar-beet canopies of which the plant cover fraction was augmented by 1% from 3% to the statistical maximum of 4%. On the day of the fourth overpass (30.7.92), 10 days after the beginning of the grain harvest, the 10% cover fraction of wheat fields was set to 0%, and a 10% stubble field cover was assumed. During autumn the photosynthetically active grass cover was reduced to 8% and compensated by a

**Table 2** Dates of phenological development, dates of the satellite overpasses, and land surface cover fraction of the Rheinhessen test area (*Vi* vine, *Gr* grass, *Wh* wheat, *Sb* sugar beet, *Ry* rye, *Fa* fallow, *Co* concrete, *As* asphalt, *So* soil, *Sf* stubble field (as an auxiliary quantity). The statistical values are given in the top part of the table. In the following lines (third column) the cover fractions manipulated by phenological information are specified for the dates of the satellite overpasses. The fourth column contains the synthetic spectral reflectances assumed for channels 1 and 2, $r^{Ch1}$ and $r^{Ch2}$, the synthetic normalized difference vegetation index, NDVI, and the vegetation cover fraction, $\sigma$ (*NOAA* National Oceanic and Atmospheric Administration)

| Beginning of phenological developments | Date of NOAA-11 overpass | Cover fraction (%) | Synthetic values |
|---|---|---|---|
| | | Vi Gr Wh Sb Ry Fa Co As So (Sf) | $r^{Ch1}$ $r^{Ch2}$ NDVI $\sigma$ |
| | | (Statistical values) | (Statistical values) |
| | | 50 20 10 04 02 01 01 02 10 00 | 0.08 0.27 0.56 0.86 |
| 02.05.92: winter wheat shoot development, 06.05.92: vine-leaf unfolding | 18.05.92 | 30 20 10 03 02 01 01 02 31 00 | 0.10 0.26 0.44 0.65 |
| 05.06.92: sugar-beet canopy closing, | 15.06.92 | 50 20 10 04 02 01 01 02 10 00 | 0.09 0.27 0.51 0.86 |
| 14.06.92: vine full flowering | 30.06.92 | 50 20 10 04 02 01 01 02 10 00 | 0.09 0.27 0.51 0.86 |
| 20.07.92: grain harvest | 30.07.92 | 50 20 00 04 02 01 01 02 10 10 | 0.09 0.27 0.50 0.76 |
| | 09.08.92 | 50 20 00 04 00 01 01 02 10 12 | 0.09 0.27 0.49 0.74 |
| 20.09.92: sugar-beet harvest, | 27.09.92 | 50 15 00 00 00 01 01 02 16 15 | 0.10 0.26 0.43 0.65 |
| 12.10.92: vine-leaf discoloration | 13.10.92 | 50 15 00 00 00 01 01 02 16 15 | 0.10 0.26 0.43 0.65 |
| 17.10.92: vine leaf fall, | 02.01.93 | 05 08 03 00 01 01 01 02 67 12 | 0.16 0.24 0.21 0.17 |
| 19.10.–15.11.92: grain emergence | 02.03.93 | 05 08 03 00 01 01 01 02 67 12 | 0.16 0.24 0.21 0.17 |
| | 09.03.03 | 05 08 03 00 01 01 01 02 67 12 | 0.16 0.24 0.21 0.17 |
| (Interseasonal values) | 20.03.93 | 05 14 08 00 01 01 01 02 62 06 | 0.15 0.24 0.25 0.28 |
| 16.04.93: sugar-beet emergence, | 28.04.93 | 15 20 10 01 02 01 01 02 48 00 | 0.12 0.25 0.36 0.48 |
| 19.04.93: winter-wheat shoot development, 26.04.93: vine leaf unfolding | 29.04.93 | 15 20 10 01 02 01 01 02 48 00 | 0.12 0.25 0.36 0.48 |

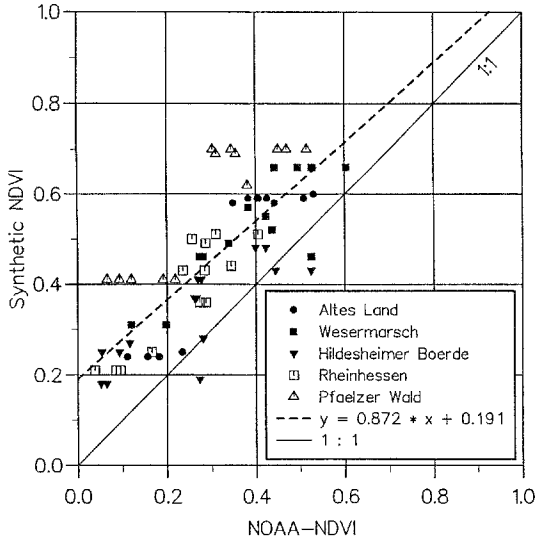


**Fig. 3** Comparison between area-averaged normalized difference vegetation indices of the National Oceanic and Atmospheric Administration satellite (NOAA-NDVIs) and area-averaged synthetic canopy NDVIs for all the five test areas on 18 selected days of satellite overpasses. The linear regression line is also plotted

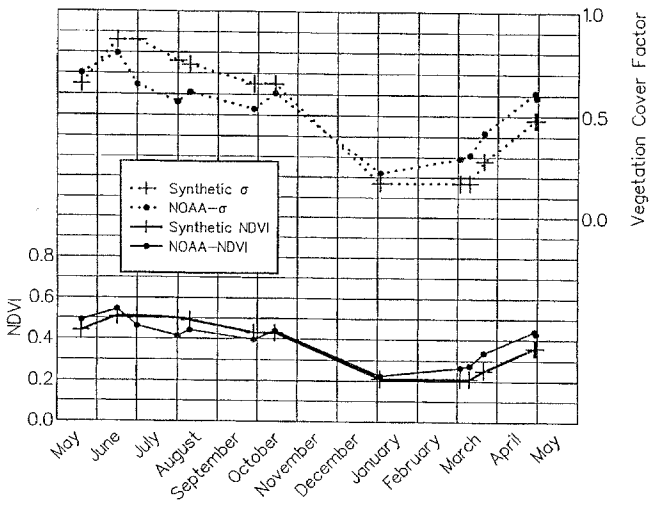


**Fig. 5** Annual course (May 1992–April 1993) of the synthetic canopy NDVI (from Table 2) and corrected area-averaged NDVI as measured by the NOAA-11 satellite (bottom) and temporal development of the synthetic $\sigma$-data (from Table 2) and area-averaged vegetational cover fraction deduced from NOAA-AVHRR data (top) for the Rheinhessen test area

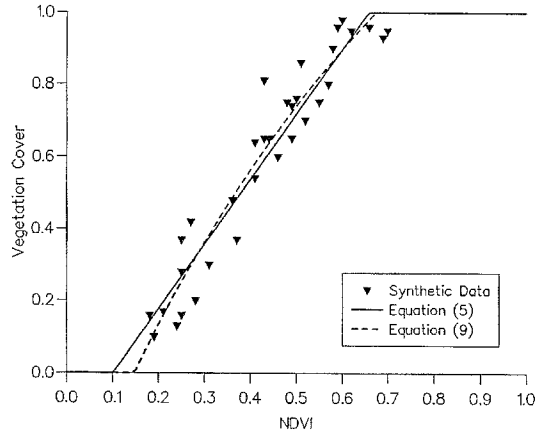


**Fig. 4** Empirical functional dependence between the synthetic NDVI and the synthetic vegetational cover fraction, $\sigma$, after Eqs. (5) and (9). The data set contains data of all the five test areas

mixture of soil and stubble field covers due to yellowing and browning during winter dormancy. When the green-up phase began after the winter months, the various vegetation covers were augmented up to their statistical maximum, while the auxiliary values (stubble field, soil) were reduced.

The results of this classification, e.g. the assessed temporal courses of weighted synthetic land-surface reflectance data for the wavelength intervals of channels 1 and 2, the assessed synthetic NDVI and the assessed vegetation cover portion, are given in the last column of Table 2. In addition, of the synthetic NDVI curves plotted in Fig. 2, the additional three NOAA curves represent: (1) the mean value taken over the whole test area covered by 9 pixels including border zones; (2) the absolute minimum of NDVI inside this area (1 pixel); and (3) the absolute area maximum of NDVI (1 pixel). The curves show similar behaviour comparable to the variation of the synthetically derived NDVI. However, there is an offset of about 0.15 units between the area-averaged NOAA-NDVIs and the synthetic values, which corresponded to the mean difference averaged over the five test areas (see Hansing and Wittich 1993). To find a simple overall formula to reduce the offset of our data, the synthetically derived NDVIs of all five test areas are compared with NOAA-NDVI analogues in Fig. 3. The equation $NDVI_{syn}=A*NDVI_{NOAA}+B$ can be made to fit the NOAA observations reasonably well when $A=0.872$ and $B=0.191$.

In Fig. 4 the synthetically derived area-averaged NDVI values of all the five test areas are plotted against the corresponding synthetic vegetation cover factors, $\sigma$, for the dates of the satellite's overpasses. A linear regression analysis of Eq. (5) resulted in $a=1.795$ and $b=-0.182$ ($r^2=0.95$) giving a lower extrapolated threshold for NDVI of $NDVI_{\sigma=0}=0.10$ and an upper one of $NDVI_{\sigma=1}=0.66$. The non-linear regression of Eq. (9) resulted in $c=0.312$, $d=0.046$, $e=0.088$ and $f=0.105$ ($r^2=0.98$) with extrapolated thresholds of $NDVI_{\sigma=0}=0.15$ and $NDVI_{\sigma=1}=0.68$. Because there are only minor differences between Eqs. (5) and (9) ($|\Delta\sigma|<0.06$) in the data range of $0.18 \leq NDVI \leq 0.69$, in a first approximation the vegetation cover fraction was adequately described by the linear equation (Eq. 5).

In Fig. 5 the annual course of the vegetation cover fraction, $\sigma$, deduced from average offset-corrected NOAA-11-NDVI values for the Rheinhessen test area on the basis of Eq. (5) is compared with synthetic terrestrial data taken from Table 2. Additionally, the annual course of the offset-corrected and area-averaged

NOAA-11-NDVI and of the synthetic NDVI, also from Table 2, are included. As is to be expected, the temporal values of the vegetation cover fraction follow those of NDVI.

## Discussion

The plant cover fraction as a synonym for the area-averaged biophysical activity at the land surface was analysed in relation to multispectral data. Firstly, the NOAA-NDVI was compared with land-surface NDVIs deduced for five test areas and the offset was corrected by a simple linear relation. In agreement with our results, Bolle et al. (1991) have found that the NOAA-NDVI remains below the ground-based measured values due to atmospheric effects (e.g. turbidity of the atmosphere, residual subscale cloud contamination of pixels) and bidirectional reflectance at the surface. These findings have been confirmed by Myneni et al. (1992), who have shown that atmospheric perturbations damp the satellite NDVI to values below the canopy NDVI. Additionally, NOAA-7 NDVI responses of dense green-leaf vegetation yield maximum values of 0.5, as reported by Holben (1986), compared to our synthetic value of c. 0.7. This offset of the data is in agreement with the results of Holben's theoretical simulation, showing a discrepancy of $\Delta$NDVI approximately equal to 0.2 between NDVIs affected by an atmosphere with heavy aerosol mass loading and those affected by a clean Rayleigh atmosphere.

In the second step of our study the validity was tested of a linear and non-linear relation between the vegetation cover factor and the spectral reflectance, as given by the NDVI. The empirical analysis showed in a first approximation that the linear expression was adequate to describe $\sigma$ over a wide distributional range of heterogeneous vegetation densities. In agreement with our results Carlson et al. (1990) have mentioned that the upper limit of NDVI for dense vegetation is in the range of 0.5–0.8 depending on vegetation type, age and leaf water content, while for bare soils the NDVI tends to vary between –0.1 and +0.2. Phulpin et al. (1990) have also obtained a linear trend in $\sigma$-NDVI values, with $NDVI_{\sigma=0}$ approximately equal to 0.15 and $NDVI_{\sigma=1}$ approximately equal to 0.7. This agrees with our findings based on Eqs. (5) and (9), i.e. $NDVI_{\sigma=1}$ equal to 0.66–0.68 for solid vegetation cover and $NDVI_{\sigma=0}$ equal to 0.10–0.15 as a threshold for non-vegetated surfaces and non-living organic matter. Kustas et al. (1993) have also found a rough linear trend in their $\sigma$-vegetation index relationship based on aircraft spectral data. Ormsby et al. (1987) have related Landsat-NDVIs to the fractional vegetation cover. Their linear regression analysis showed a strong correlation between both parameters while Myneni et al. (1992) have pointed out that the slope of the increase of NDVI with respect to ground cover depends on the leaf area index and on soil colour.

The empirical $\sigma$-NDVI relationships of Eqs. (5) and (9) can be used for quick first-order estimates. In detail, however, the vegetation cover problem is more complex because the scattering coefficients for the leaves and the soil, the leaf-area index, the leaf angle distribution and the angle of incident radiation affect the NDVI. Further research is required to improve the algorithms to reduce the errors in estimates (see the offset in Fig. 2) by more sophisticated correction methods.

**Acknowledgements** The authors are grateful to J. Asmus, W. Benesch and H. Knottenberg for providing the NOAA-AVHRR data and facilitating handling of the data.

## References

Blümel K, Bolle H-J, Eckardt M, Lesch L, Tonn W (1988) Der Vegetationsindex für Mitteleuropa 1983–1985 (The vegetation index for Central Europe 1983–1985). Institut für Meteorologie, Berlin

Bolle H-J, Katergiannakis U, Tonn W (1991) Der Vegetationsindex 1989 für Mitteleuropa anhand zweier ausgewählter Beispiele (The vegetation index of 1989 for Central Europe on the basis of two selected examples). Wetter und Leben 43: 115–135

Bowker DE, Davis RE, Jones WT, Myrick DI, Stacy K (1985) Spectral reflectances of natural targets for use in remote sensing studies. NASA Reference Publication 1139, Washington

Buschmann C, Stützel M (1993) Private communication

Carlson TN, Perry EM, Schmugge TJ (1990) Remote estimation of soil moisture availability and fractional vegetation cover for agricultural fields. Agric Forest Meteorol 52:45–69

Deardorff JW (1978) Efficient prediction of ground surface temperature and moisture, with an inclusion of a layer of vegetation. J Geophys Res 83 C4:1889–1903

Hansing O, Wittich K-P (1993) Verifikation des aus NOAA-11-Satellitenbilddaten abgeleiteten Vegetationsindexes für fünf Regionen Westdeutschlands (Validation of the vegetation index deduced from NOAA-11 satellite data for five regions in western Germany). DWD-intern 56, Deutscher Wetterdienst, Offenbach

Holben BN (1986) Characteristics of maximum-value composite images from temporal AVHRR data. Int J Remote Sensing 7:1417–1434

Huss J (1985) Luftbildmessung und Fernerkundung in der Forstwirtschaft (Aerial photographs and remote sensing in forestry). Wichmann, Karlsruhe

Justice CO, Townshend JRG, Holben BN, Tucker CJ (1985) Analysis of the phenology of global vegetation using meteorological satellite data. Int J Remote Sensing 6:1271–1318

Kadro A (1981) Untersuchung der spektralen Reflexionseigenschaften verschiedener Vegetationsbestände (Study of the spectral reflectivities of different crops). PhD Thesis, University of Freiburg

Kustas WP, Schmugge TJ, Humes KS, Jackson TJ, Parry R, Weltz MA, Moran MS (1993) Relationships between evaporative fraction and remotely sensed vegetation index and microwave brightness temperature for semiarid rangelands. J Appl Meteorol 32:1781–1790

Manzi AO, Planton S (1994) Implementation of the ISBA parametrization scheme for land surface processes in a GCM – an annual cycle experiment. J Hydrol 155:353–387

Myneni RB, Asrar G, Tanre D, Choudhury BJ (1992) Remote sensing of solar radiation absorbed and reflected by vegetated land surfaces. IEEE Trans Geosci Remote Sensing 30:302–314

Ormsby JP, Choudhury BJ, Owe M (1987) Vegetation spatial variability and its effect on vegetation indices. Int J Remote Sensing 8:1301–1306

Phulpin T, Noilhan J, Stoll M (1990) Parameters estimates of a soil-vegetation model using AVHRR data. Proceedings of the 4th AVHRR data users meeting, Rothenburg, Germany, 5–8 Sept. 1989. EUMETSAT, Darmstadt, EUM P 06, pp 125–129

Sellers PJ (1985) Canopy reflectance, photosynthesis and transpiration. Int J Remote Sensing 6:1335–1372

Sellers PJ (1987) Canopy reflectance, photosynthesis and transpiration. II. The role of biophysics in the linearity of their interdependence. Remote Sensing Environ 21:143–183

Sellers PJ, Berry JA, Collatz GJ, Field CB, Hall FG (1992) Canopy reflectance, photosynthesis and transpiration. III. A reanalysis using improved leaf models and a new canopy integration scheme. Remote Sensing Environ 42:187–216

Szasz G (1986) Die Bedeutung der Fernerkundung in der großräumigen phänologischen Betrachtung (The significance of remote sensing in the phenological observation of a large area). Sonderheft zum Internationalen Phänologie-Symposium an der Universität für Bodenkultur, Wien, 17–20 Sept. 1986. Arboreta Phaenologica 31, pp 111–119